BEFORE THE BAR:
KINEMATIC DETECTION OF A SPHEROIDAL METAL-POOR BULGE COMPONENT

Andrea Kunder[1], R. M. Rich[2], A. Koch[3], J. Storm[1], D. M. Nataf[4], R. De Propris[5], A. R. Walker[6], G. Bono[7,8], C. I. Johnson[9], J. Shen[10], Z.-Y. Li[10],
accepted by ApJ Letters

ABSTRACT

We present 947 radial velocities of RR Lyrae variable stars in four fields located toward the Galactic bulge, observed within the data from the ongoing Bulge RR Lyrae Radial Velocity Assay (BRAVA-RR). We show that these RR Lyrae stars exhibit hot kinematics and null or negligible rotation and are therefore members of a separate population from the bar/pseudobulge that currently dominates the mass and luminosity of the inner Galaxy. Our RR Lyrae stars predate these structures, and have metallicities, kinematics, and spatial distribution that are consistent with a "classical" bulge, although we cannot yet completely rule out the possibility that they are the metal-poor tail of a more metal rich ([Fe/H]~-1 dex) halo-bulge population. The complete catalog of radial velocities for the BRAVA-RR stars is also published electronically.

Subject headings: Galaxy: bulge; Galaxy: kinematics and dynamics; Galaxy: structure; halo

1. INTRODUCTION

The majority of massive galaxies ($> 10^9 M_\odot$), similar to the Milky Way, have a distinct rise in surface brightness above the disk, referred to as a bulge (Fisher & Drory 2011). Galaxy bulges are observed to either rotate rapidly like a disk, and are generally referred to as pseudobulges, or they are dominated by random motions and are therefore pressure supported by a central velocity dispersion. This latter type is referred to as a classical bulge (e.g., Kormendy & Illingworth 1982). That not all bulges are alike suggests that the bulge type of a galaxy carries significance for the galaxy's evolutionary history, such as its merger history and star formation efficiency (e.g., Martig et al. 2012; Obreja et al. 2013; Fiacconi et al. 2015). The properties of the bulge in our Galaxy are therefore, a fundamental parameter with which to understand the formation of the Milky Way.

The first wide-area spectroscopic surveys of the Milky Way bulge have shown that it consists of a massive bar rotating as a solid body (Rich et al. 2007; Kunder et al. 2012; Ness et al. 2013; Zoccali et al. 2014). The internal kinematics of these stars are consistent with at least 90% of the inner Galaxy being part of a pseudobulge and lacking a pressure supported, classical-like bulge (Shen et al. 2010; Ness et al. 2013). Recent studies have indicated a bimodal nature of bulges – that two bulge populations, likened to classical and pseudo-bulges, can exist within a galaxy, with differences being in the relative proportions of the two (Obreja et al. 2013; Fisher & Drory 2016). There has accordingly been considerable debate about whether there is room for a classical component in the bulge (Babusiaux et al. 2010; Zoccali et al. 2008).

The oldest and most metal poor stars (which may trace the dark matter) are thought to be found in the center of the Galaxy – in the bulge but not sharing its kinematics and abundance patterns (Tumlinson 2010). Therefore, perhaps the greatest possibility of uncovering a classical component would be within the metal-poor bulge stars. Unfortunately, spectroscopic surveys studying thousands of giants and red clump stars in the bulge have found that metal-poor stars in the bulge are rare, greatly limiting the use of metal-poor stars to uncover and probe a possible classical bulge component (Ness et al. 2013; Casey & Schlaufmann 2015; Howes et al. 2015; Koch et al. 2016). Perhaps the easiest identifiable old, metal-poor bulge population are those horizontal branch stars that pulsate as RR Lyrae stars (RRLs). Since the absolute brightness of RRLs are known to within $\sim$10%, the discovery of a significant population of RRLs toward the bulge permitted the first distance determination to the Galactic center from a stellar population (Baade 1946).

In this paper, we report on the kinematics of a large sample of these stars in the Galactic bulge field. Our sample consists of RRLs with Galactocentric distances within $\sim$10% of the distance of the Sun to the galactic center, so our sample represents the typical "bulge" RRL population.

2. OBSERVATIONS AND RADIAL VELOCITY

Observations were performed using the AAOmega multi-fiber spectrograph on the Anglo-Australian Tele-

[1] Leibniz-Institut für Astrophysik Potsdam (AIP), An der Sternwarte 16, D-14482 Potsdam, Germany
[2] Department of Physics and Astronomy, University of California at Los Angeles, Los Angeles, CA 90095-1562, USA
[3] Physics Department, Lancaster University, Lancaster LA1 4YB, UK
[4] Research School of Astronomy and Astrophysics, The Australian National University, Canberra, ACT 2611, Australia
[5] Finnish Centre for Astronomy with ESO, University of Turku, 2150 Turku, Finland
[6] Cerro Tololo Inter-American Observatory, National Optical Astronomy Observatory, Casilla 603, La Serena, Chile
[7] Dipartimento di Fisica, Universita di Roma Tor Vergata, vi a Della Ricerca Scientifica 1, 00133, Roma, Italy
[8] INAF, Rome Astronomical Observatory, via Frascati 33, 00040, Monte Porzio Catone, Italy
[9] Harvard-Smithsonian Center for Astrophysics, Cambridge, MA 02138
[10] Key Laboratory for Research in Galaxies and Cosmology, Shanghai Astronomical Observatory, Chinese Academy of Sciences, 80 Nandan Road, Shanghai 200030, China

scope (AAT) on May 2013, June 2013, June 2014 and August 2015, in dual beam mode centered on 8600Å, with the 580V and 1700D gratings to probe the Calcium Triplet (NOAO PropID: 2014A-0143; PI: A. Kunder and NOAO PropID: 2015B-071; PI: A. Kunder). This covers the wavelength regime of about 8300Å to 8800Å at a resolution of R∼10,000. Exposure times were between one to two hours, and in general there are between 2 and 5 epochs for each RRL. The 2013 observations were carried out in conjunction with a bulge survey designed for detached red giant eclipsing binary twins (AAT: 2013A-05; PI: D. Nataf). Extra fibers were available and resourcefully allocated to 95 bulge RRLs, and these RRLs have up to 15 epochs of observations.

The OGLE-III catalogue of RRLs (Pietrukowicz et al. 2012) was used to select the targets. We observed all bulge fundamental mode RRLs (RR0 Lyrae stars) that were free of a companion within a 2 arc second radius in our four fields. These have been phased by the stars known period, and over-plotted with the radial velocity template from Liu (1991) (Figure 1). This template is scaled using a correlation between the amplitudes of velocity curves and light curve:

$$A_{rv} = \frac{40.5 \times V_{amp} + 42.7}{1.37} \quad (1)$$

as shown in Liu (1991). Because the I-amplitude of the OGLE stars is known much more precisely than the V-amplitude, we use the relation $V_{amp} = I_{amp}$ x 1.6 to find each stars V-amplitude (see e.g., Table 3 in Kunder et al. 2013). The so-called "projection factor" $p= 1.37$ is necessary because Liu (1991) uses pulsation velocities, which are related to observed radial velocities as $v_{obs} = v_{puls}/p$. The projection factor p can range from 1.31 to 1.37 (Liu 1991; Kovacs 2003), and we adopted $p= 1.37$ as in Sesar (2012).

Due to our sampling techniques, almost all of our stars have at least two spectra at different phases, which facilitates the fitting of a radial velocity curve to the measurements. The zero-point in phase is fixed using the time of maximum brightness as reported by OGLE-IV (Soszy'nski et al. 2014) and the pulsation curve is shifted in radial velocity until it matches the observations. More weight is given to points that fall between $\phi =0.0$ - 0.6, as this is where the uncertainty in the radial velocity shape of the template is minimised (see, e.g., Fig. 1 in Sesar 2012). More weight is also given to the observations with a higher signal-to-noise, which also generally occurs between $\phi =0.0$ - 0.6. The star's time-averaged velocity is determined by finding the velocity at $\phi_{obs}=0.38$ (Liu 1991).

We use 24 RRLs with well derived radial velocities to investigate how 2-3 epochs per light curve affect our center-of-mass radial velocities. The 24 RRLs are listed in Table 1, and span a wide range of metallicities, pulsation periods and amplitudes. Because these 24 RRLs have individual radial velocity uncertainties that are ∼1 km s^{-1}, we first assign each radial velocity measurement a Gaussian uncertainty distribution of 4 km s^{-1}, to simulate the typical errors from the observed BRAVA-RR observations. We then use the Liu (1991) template and decrease the number of epochs from ∼100 to 2 and measure how the center-of-mass radial velocity changes.

In general, the center-of-mass radial velocity changes by ∼2 km s^{-1} or less; only in the unusual cases where there were no epochs between $\phi =0.0$ - 0.6, but instead the observations fell on the rising branch at phases greater than 0.85, did the center-of-mass radial velocity change by ∼5 km s^{-1}.

Similar results have been shown previously; for example, Jeffery et al. (2007) showed that center-of-mass radial velocities have a typical uncertainty of ±1.5 km s^{-1} for variables observed at least three times when using the Liu (1991) template. A visual inspection of the radial velocity curves of the 63 BRAVA-RR stars with 10 or more epochs of observations also indicates that the Liu (1991) template is sufficient to within 5 - 10 km^{-1} to obtain a center-of-mass radial velocity. Indeed, it is impressive how well the radial velocity template fits to the diverse RRLs listed in Table 1. We note that 87% of our BRAVA-RR stars have 3 or more epochs of observations, making it statistically unlikely that the BRAVA-RR stars do not have observations in the regime where the template most accurately aligns with the observed radial velocity measurements. Therefore, our center-of-mass radial velocity uncertainties are 5-10 km s^{-1}.

Figure 1 shows example pulsation curves for the RRLs – in particular, we show is those with the most extreme radial velocities to illustrate this is a kinematically hot population. Table 2 gives the OGLE-ID (1), the RA (2) and Dec (3) as provided by OGLE, the star's time-average velocity (4), the number of epochs used for the star's time-average velocity (5), the period of the star (6), the V-band magnitude (7), the I-band magnitude (8) and the I-band amplitude (9) as calculated by OGLE, and lastly the photometric metallicity from the OGLE I-band light curve (10).

3. DISCUSSION

3.1. *Rotation curve*

From spectroscopic observations of 947 RRLs in four 3 sq. deg. fields located toward the bulge we plot the mean radial velocity and velocity dispersion for RRLs as a function of position (galactic latitude and longitude) in Figure 2. These are found to be radically different from the trends traced by the more metal-rich red giants in the BRAVA and GIBS surveys (Kunder et al. 2012; Zoccali et al. 2014) as the RRLs show null rotation and hot (high velocity dispersion) kinematics. In the ARGOS survey one observes a slowly-rotating metal-poor population (Ness et al. 2013), which is hypothesized to arise from stellar contamination from disk and halo stars, as it is only seen at high galactic latitude. In contrast, our stars are at low galactic latitudes and their more certain distance estimates indicate they are within 1 kpc of the Galactic center, where the surface-density of bulge stars is usually dominant compared to the disk and halo. We conclude that we are tracing an older, more spheroidal component in the inner Galaxy that may be likened to a classical bulge.

3.2. *Metallicity distribution*

The [Fe/H] metallicity distribution in our sample spans three orders of magnitude, with spectroscopic metallicities derived from the Calcium Triplet 8498 Å line (Wallerstein et al. 2012) ranging from −2.5 to super-
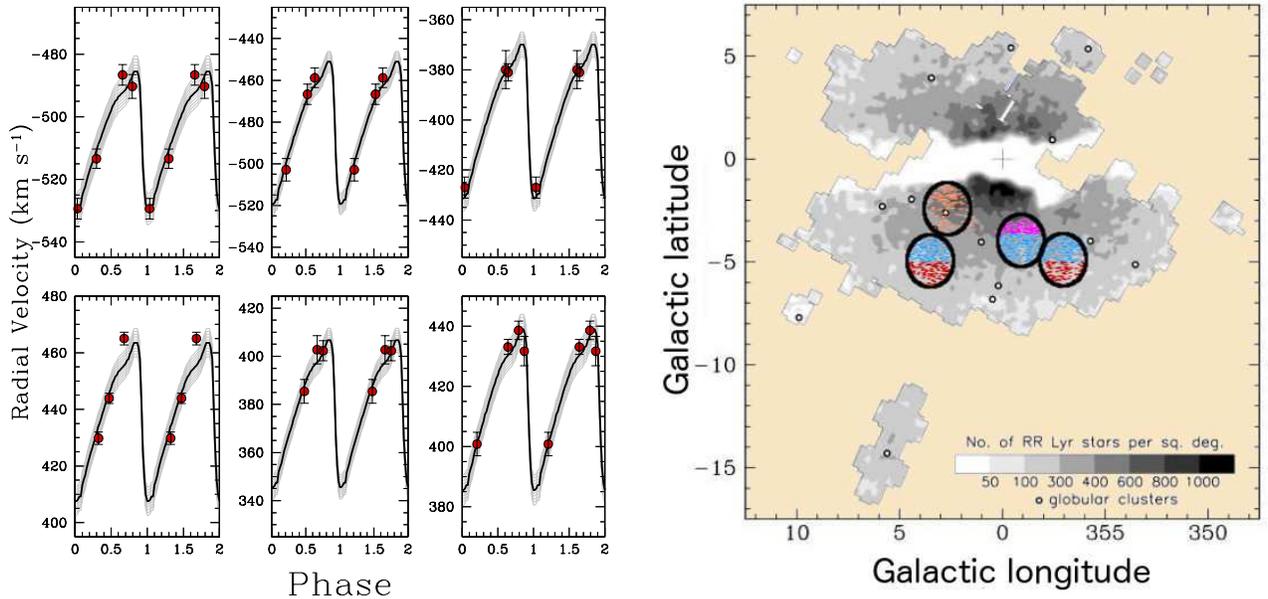
FIG. 1.— *Left:* The line-of-sight radial velocity versus pulsational phase for a sample of BRAVA-RR observations; over-plotted is a fundamental mode RRL radial velocity template, scaled by its V-amplitude (see Equation 1, and also Liu 1991). The grey shaded area shows the 5 km s^{-1} uncertainty in the template, which is also the typical uncertainty in our individual radial velocity measurements. *Right:* The spatial location of the OGLE RRLs in the Galactic bulge, with the RRLs presented here shown as bold symbols. The observed RRLs are color coded to designate the strips of latitude they are separated into, with which to obtain their rotation curve (see Figure 2).

solar metallicities, peaking at [Fe/H]~-1 dex. Therefore, as shown previously (Walker & Terndrup 1991), the bulge field RRLs are on average $\sim$1 dex more metal-poor than 'normal' bar stars, yet some of the bulge field RRLs have metallicities that overlap in abundance with the bar population. The bulge field RRLs are also more metal-rich than the stellar halo (e.g., An et al. 2013), although the metallicity gradient observed in the field RRLs is consistent with an inner bulge-halo at distances closer to the Galactic center being more metal-rich (Suntzeff et al. 1991).

None of the bulge field RRL are extremely metal poor, in contrast with what is predicted from a very old inner-halo (Tumlinson 2010; Howes et al. 2015) there is presently no indication for many stars in our sample with [Fe/H] < -3, although the evolutionary tracks for such metal poor stars may make it less likely for them to traverse through the instability strip, thus becoming an RR Lyrae star (e.g., Lee et al. 1994, see their Figure 1). The large metallicity spread is suggestive of multiple populations within the bulge field RRL sample (Lee et al. 2015). In Figure 2, it is clear that the metal-rich RRLs have a smaller dispersion compared to the more metal-poor stars, which indicates there were likely various RRL formation mechanisms in the bulge. This might plausibly be related to the two distinct bulge field RRL sequences in the period-amplitude diagram (Pietrukowicz et al. 2015) as well as the suggestion that only in the most central part (inner 1 kpc) of the bulge do the RRLs exhibit a weak bar-like substructure (Pietrukowicz et al. 2012; Dékány et al. 2013).

We note that the BRAVA-RR spectroscopic metallicities are still being finalized, and this will be the topic of a subsequent BRAVA-RR paper. Therefore throughout this paper we use photometric metallicities obtained from a linear metallicity relationship in the pulsational period and phase difference between the first and third harmonic ϕ_{31} (where $\phi_{nm} = m\phi_n - n\phi_m$) in a Fourier decomposition of the OGLE I-band lightcurves (Smolec 2005). These photometric metallicites are placed on the Carretta et al. (2009) metallicity scale. The plots, however, does not change significantly when using our preliminary CaT abundances.

3.3. *Mass estimate*

We can estimate the mass of the 'old' inner Galaxy component by comparing the relative numbers of red clump giants (metal rich horizontal branch stars) and RRLs in the OGLE-III survey (Pietrukowicz et al. 2012; Nataf et al. 2013). Here we assume that all the red clump stars are part of the rotating bar, whereas all the RRL are part of a non-rotating component (e.g., a classical bulge). We also presume that RRLs have the same lifetime as red clump stars and were formed from stellar populations with the same IMF as the red clump stars. The kinematically hot component we recover in this paper then amounts to $\sim$1% of the total central mass. A similar mass is calculated from the fuel consumption theorem (Renzini & Buzzoni 1986), assuming again all the RRL are part of a non-rotating component and have a narrow range in age. This is broadly consistent with current bulge formation models, which predict that no more than $\sim$5% of a merger-generated bulge, which is slowly rotating and dispersion-supported, may exist within the Milky Way bulge (Shen et al. 2010; Ness et al. 2013; Di Matteo et al. 2015). Although such a small mass may pose a challenge in understanding how this central component could remain stationary in the much more massive bar potential (Saha & Gerhard 2013), some dynamical studies do suggest that a hot pop-

ulation is only weakly affected, if at all, by the bar dynamics (Minchev et al. 2012).

3.4. *Interpretation*

Our velocities rule out that possibility that the majority of RRL in the direction of the bulge are part of the bar. Given the ages of RRLs (Walker 1989; Lee et al. 1992), this indicates that the inner Galaxy component traced out by the BRAVA-RR stars is at least ∼1 Gyr older than the dominant bar population.

It may be that the RRL stars toward the bulge are actually an inner halo-bulge sample, as originally speculated in the early 1990s (e.g., Minniti 1994) and as at least one RRL orbit toward the Galactic bulge seems to indicate (Kunder et al. 2015). However, the velocity dispersion of the bulge RRLs is ∼10 km s^{-1} larger than that seen in both the local RRL halo sample (Layden 1994; Beers et al. 2000) and from other halo star samples (e.g. Battaglia et al. 2006; Brown et al. 2009). In fact, we are not aware of any other stellar population in the galaxy with a larger velocity dispersion than that of the BRAVA-RR stars. The decrease in velocity dispersion with metallicity (seen in Figure 2 and Figure 3) is also characteristic of stars located in the bulge regions (e.g., Rich et al. 1990; Johnson et al. 2011; Babusiaux et al. 2010). In contrast, the velocity dispersion of halo stars either does not change (e.g., Norris 1986), or does not change as significantly (e.g., Chiba & Beers 2000; Kafle et al. 2013) as a function of metal-abundance. A comparison of velocity dispersion with [Fe/H] for the BRAVA-RR stars and for the halo RRL star sample of Layden (1994) and Beers et al. (2000) is shown explicitly in Figure 3 (left panel). If the RRL stars toward the bulge are an inner halo-bulge population, this component would be the most metal-rich halo population identified in the Galaxy, with a mean [Fe/H]∼−1 dex, compared to the inner halo ([Fe/H]∼−1.6 dex) and the outer halo ([Fe/H]∼−2.2 dex) (e.g., An et al. 2013).

Recent studies have indicated that a kinematically warmer component associated with the Galactic thick disk could be present in the bulge, and would not be part of the bar structure traced out by the majority of the bulge red giants (e.g., Di Matteo et al. 2015). We therefore verified if the bulge RRLs have properties that could link them to the thick disk. However, as seen in Figure 3 (left panel), OGLE-II proper motions (Sumi et al. 2004) of our observed RRLs set them apart from that of the disk, not surprising, as it is known that only ∼20% of RRLs in the Milky Way reside in the (thick) disk (Layden 1995). Figure 3 also illustrates how the period distribution of the bulge field RRLs is shifted to longer periods in comparison to the RRL kinematically identified by Layden (1994, 1995) as belonging to the thick disk. Although the local thick disk sample is small (37 stars total), from an RRL pulsational tagging stand point it appears unlikely that the BRAVA-RR component was formed in a similar manner to that of the Milky Way thick disk.

4. CONCLUSIONS

It has proven extremely difficult to disentangle the formation history of the inner Galaxy. RRLs are the only luminous evolved stars for which it is possible to place a time stamp: these stars are older than 11 Gyr (Walker 1989). It appears that in the RRL population toward the Galactic bulge, we can observe a distinct stage of the formation of the inner Galaxy that was antecedent to the formation of the bar. This is in agreement with an axisymmetric geometry described using near-infrared VVV observations (Dékány et al. 2013), and is in contrast to the view provided from optical OGLE photometry in which the RRLs appear to follow the elongated spatial distribution of the bar (Pietrukowicz et al. 2015).

The different kinematics of the "bulge" field RRLs and the majority of the bulge giants supports the claim that galaxies may harbor two populations in the inner Galaxy, which may be likened to classical and pseudobulges, with differences being with the fraction of the two (Obreja et al. 2013). Within the RRLs population toward the direction of the bulge, we can probe an early epoch inner Galaxy that was formed before the massive disk secularly evolved into the bar. Detailed models of the halo, thick disk and bulge components ∼1 kpc from the Galactic center, an understanding of the elemental abundances of the RRLs, as well as a large sample of accurate proper motions for our BRAVA-RR stars, will help distinguish if the "bulge" RRLs reside in a classical-like bulge, or are part of a different Milky Way component, such as a metal-rich inner halo-bulge.
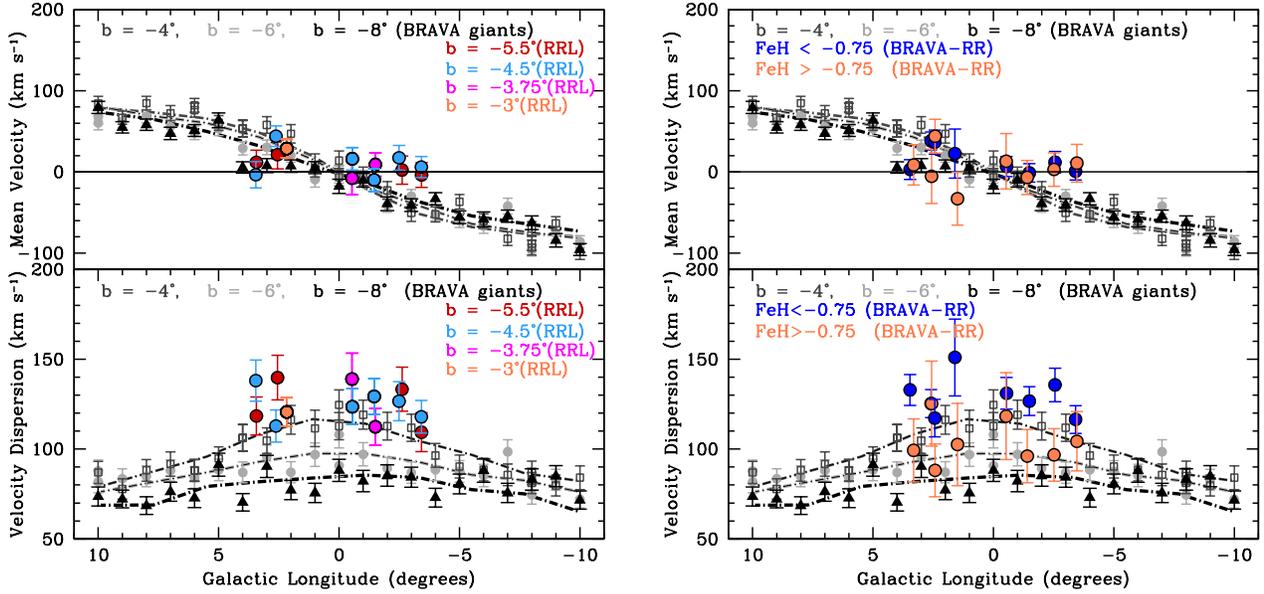
FIG. 2.— *Left:* The velocity dispersion profile (bottom) and rotation curve (top) for the RRLs we have already observed compared to that of the BRAVA giants at $b = -4°$, $-6°$, and $-8°$ strips (Kunder et al. 2012). The bulge model showing these observations are consistent with a bulge being formed from the disk is represented by the dashed lines (Shen et al. 2010). The RRLs have kinematics clearly distinct from the bulge giants, and are a non-rotating population in the inner Galaxy. *Right:* The velocity dispersion profile (bottom) and rotation curve (top) for the RRLs seperated into metal-rich ([Fe/H]>−0.75) and metal-poor ([Fe/H]<−0.75) stars. The more metal-rich RRLs have metallicities that overlap with the pseudobulge red giants, yet they still show no substantial rotation.
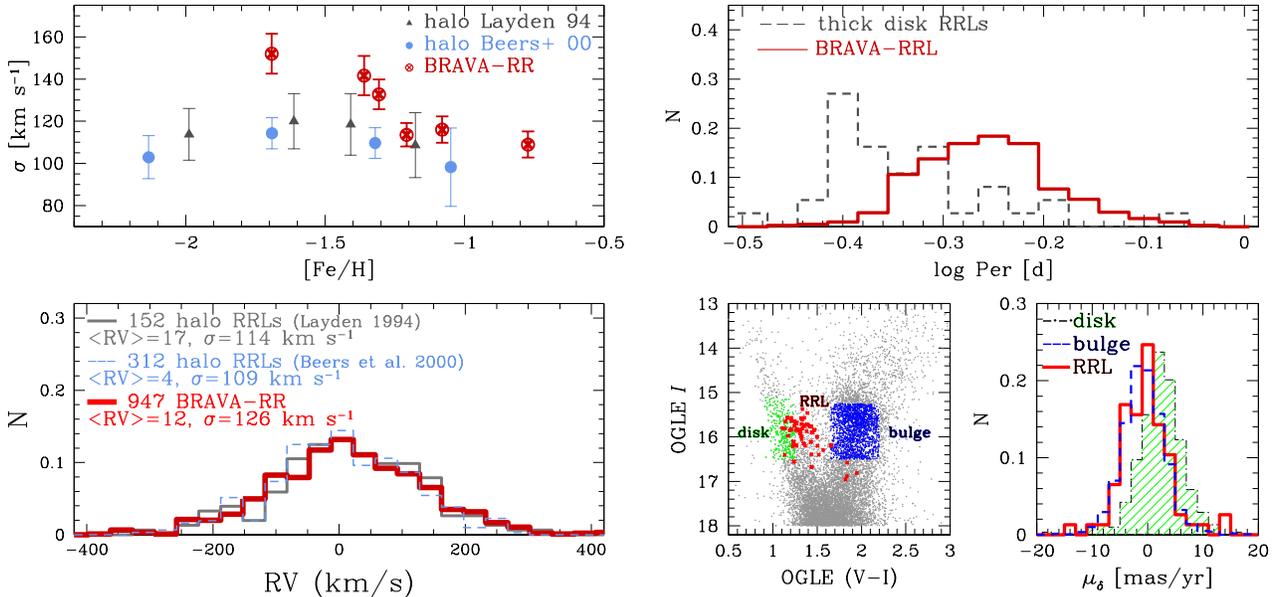

FIG. 3.— *Left top:* The velocity distribution of the BRAVA-RR stars and the halo RRLs in the Layden (1994) and Beers et al. (2000) sample as a function of [Fe/H]. *Left bottom:* The radial velocity distributions showing the kinematically selected halo RRL stars from Layden (1994), the non-kinematically selected metal-poor ([Fe/H] < −1 dex) RRL sample from Beers et al. (2000), and the BRAVA-RR stars presented here.
Right top: The period distribution of local thick disk RRLs selected kinematically by Layden (1994, 1995) compared to the period distribution of the BRAVA-RR stars. The bulge RRLs have longer periods as compared to the thick disk RRLs. *Bottom Left:* The CMD of a typical bulge field in the OGLE-II catalog showing the separation of disk (green) and bulge (blue) populations; the magnitudes and colors of the 77 BRAVA-RR stars with OGLE-II proper motions are shown as red crosses. *Bottom Right:* The histogram of the OGLE-II proper motions for the disk (green), bulge (blue), and BRAVA-RR stars (red) (see left panel). The BRAVA-RR stars follow the proper motion distribution expected for a typical bulge population.

TABLE 1
Radial velocity light curves of local RR Lyrae stars

Name	log Period (d)	[Fe/H]	Source
WY Ant	-0.240838	-1.25	Skillen et al. (1993)
X Ari	-0.186314	-2.20	Jones et al. (1987)
RR Cet	-0.257245	-1.25	Liu & Janes (1989)
UU Cet	-0.217469	-1.00	Clementini et al. (1990)
W Crt	-0.383976	-0.70	Skillen et al. (1993)
DX Del	-0.325491	-0.20	Meylan et al. (1986)
RX Eri	-0.231180	-1.40	Liu & Janes (1989)
SS Leo	-0.203186	-1.51	Fernley et al. (1990)
RV Oct	-0.243239	-1.75	Skillen et al. (1993)
V445 Oph	-0.401187	-0.39	Fernley et al. (1990)
AV Peg	-0.408518	0.00	Liu & Janes (1989)
RV Phe	-0.224454	-1.50	Cacciari et al. (1987, 1989)
BB Pup	-0.318267	-0.60	Skillen et al. (1993)
VY Ser	-0.146245	-1.80	Carney & Latham (1984)
W Tuc	-0.192305	-1.35	Clementini et al. (1990)
UU Vir	-0.322752	-0.55	Jones et al. (1988); Liu & Janes (1989)
47Tuc-V9	-0.132620	-0.71	Storm et al. (1994)
M4-V2	-0.271092	-1.30	Liu & Janes (1990)
M4-V32	-0.237240	-1.30	Liu & Janes (1990)
M4-V33	-0.211245	-1.30	Liu & Janes (1990)
M5-V8	-0.262617	-1.40	Storm et al. (1992)
M5-V28	-0.264455	-1.40	Storm et al. (1992)
M92-V1	-0.153171	-2.24	Storm et al. (1992)
M92-V3	-0.195575	-2.24	Storm et al. (1992)

TABLE 2
Radial velocities of BRAVA-RR stars

OGLE ID	R.A. (J2000.0)	Decl. (J2000.0)	$HRV_{\phi=0.38}$ (km s^{-1})	# Epochs	Period (d)	$(V)_{mag}$	$(I)_{mag}$	I_{amp}	$[Fe/H]_{phot}$
06032	17 53 15.15	-34 10 21.3	13	3	0.53840530	17.442	16.209	0.67	-0.98
06138	17 53 23.86	-34 10 48.5	-142	3	0.51685809	16.929	15.763	0.49	-0.59
06166	17 53 26.77	-34 08 58.1	-3	3	0.53398387	16.986	15.637	0.62	-1.00
06171	17 53 27.14	-33 57 53.7	59	3	0.60629585	17.541	16.006	0.27	-0.76
06197	17 53 28.89	-34 18 09.3	27	4	0.48368631	16.791	15.696	0.70	-1.08
06227	17 53 30.50	-34 24 57.0	-12	6	0.50614560	16.841	15.760	0.59	-1.15
06257	17 53 33.61	-33 55 18.0	130	3	0.55305696	17.951	16.444	0.56	-0.91
06280	17 53 35.52	-34 05 14.5	17	2	0.50637949	18.224	16.740	0.17	0.17
06377	17 53 43.29	-34 07 09.9	-191	3	0.54579032	17.606	16.186	0.56	-0.91
06382	17 53 43.89	-34 12 24.0	-219	4	0.68896691	16.840	15.674	0.63	-1.32

REFERENCES

An, D,, Beers, T., Johnson, J.A. et al. 2013, ApJ, 763, 65
Babusiaux, C. et al. 2010, A&A, 519, 77
Baade, W. 1946, PASP, 58, 249
Battaglia, G., Helmi, A., Morrison, H., Harding, P., Olszewski, E.W., Mateo, M., Freeman, K.C., Norris, J., Shectman, S.A. 2006, MNRAS, 370, 1055
Beers, T.C., Chiba, M., Yoshii, Y., Platais, I., Hanson, R.B., Fuchs, B. & Rossi, S. 2000, AJ, 119, 2866
Brown, W.R., Geller, M.J., Kenyon, S.J. & Diaferio, A. 2009, ApJ, 690, 69
Cacciari, C., Clementini, G., Prevot, L., et al. 1987, A&AS, 69, 135
Cacciari, C., Clementini, G., & Buser, R. 1989, A&A, 209, 154
Carretta, E., Bragaglia, A., Gratton, R., D'Orazi, V. & Lucatello, S. 2009, A&A, 508, 695
Carney, B. W., & Latham, D. W. 1984, ApJ, 278, 241
Casey, A.R. & Schlaufmann, K.C. 2015, ApJ, 809, 110
Chiba, M. & Beers, T.C. 2000, AJ, 119, 2843
Clementini, G., Cacciari, C., & Lindgren, H. 1990, A&AS, 85, 865
Dékány, I., Minniti, D., Catelan, M., Zoccali, M., Saito, R. K., Hempel, M. & Gonzalez, O. A. 2013, ApJ, 776, 19
Di Matteo, P. et al. 2015, A&A, 577, 1
Fernley, J. A.; Skillen, I.; Jameson, R. F., et al. 1990, MNRAS, 247, 287
Fiacconi, D., Feldmann, R. & Mayer, L. 2015, MNRAS, 446, 1957
Fisher, D.B. & Drory, N. 2011, ApJ, 733, 47
Fisher, D.B. & Drory, N. 2016, Springer Review, archiv:1512.02230
Howes, L.M. et al. 2015, Nature, 527, 484
Jeffery, E.J., Barnes, T.G., Skillen, I. & Montemayor, T.J. 2007, ApJS, 171, 512
Johnson, C.I., Rich, R.M., Fulbright, J.P., Valenti, E. & McWilliam, A. 2011, ApJ, 732, 108
Jones, R.V., Carney, B.W., Latham, D.W. & Kurucz, R.L. 1987, ApJ, 312, 254
Jones, R.V., Carney, B.W., & Latham, D.W. 1988, ApJ, 332, 206
Kafle, P. R., Sharma, S., Lewis, G. F. & Bland-Hawthorn, J. 2013, MNRAS, 430, 2973
Koch, A., McWilliam, A., Preston, G.W. 2016, A&A, 587, 124
Kormendy, J. & Illingworth, G. 1982, ApJ, 256, 460
Kovács, G. 2003, MNRAS, 342, 58
Kunder, A., Koch, A., Rich, R. M., et al. 2012, AJ, 143, 57
Kunder, A., Stetson, P., Cassisi, S., et al. 2013, AJ, 146, 119
Kunder, A., Rich, R. M., Hawkins, K. et al. 2015, ApJ, 808, 12

Layden, A. 1994, AJ, 108, 1016
Layden, A. 1995, AJ, 110, 2288
Lee, Y.-W. 1992, AJ, 104, 1780
Lee, Y.-W., Demarque, P. & Zinn, R. 1994, ApJ, 423, 248
Lee, Y.-W., Joo, S. & Chung, C. 2015, MNRAS, 453, 3906
Liu, T. 1991, PASP, 103, 205
Liu, T., & Janes, K.A. 1989, ApJS, 69, 593
Liu, T., & Janes, K.A. 1990, ApJ, 360, 561
Martig, M., Bournaud, F., Croton, D.J., Dekel, A., Teyssier, R. 2012, ApJ, 756, 26
Meylan, G., Burki, G., Rufener, F., et al., 1986, A&AS, 64, 25
Minchev, I., et al. 2012, A&A, 548, 126
Minniti, D. 1994, PASP, 106, 813
Nataf, D.M., Gould, A., Fouqué, P. et al. 2013, ApJ, 769, 88
Ness, M. et al. 2013, MNRAS, 432, 2092
Noris, J. 1986, ApJS, 61, 667
Obreja, A. et al. 2013, ApJ, 763, 26
Pietrukowicz et al. 2012, ApJ, 750, 169
Pietrukowicz et al. 2015, ApJ, 811, 113
Renzini, A. & Buzzoni, A. 1986, ASSL, 122, 195
Rich, R.M. 1990, ApJ, 362, 604
Rich, R.M., Reitzel, D.B., Howard, C.D., Zhao, H. 2007, ApJ, 658, 29
Saha, K. & Gerhard, O. 2013, MNRAS, 430, 2039
Sesar, B. 2012, AJ, 144, 114
Shen, J., Rich, R. M., Kormendy, J., et al. 2010, ApJ, 720, L72
Skillen, I., Fernley, J. A., Stobie, R. S., & Jameson, R. F. 1993, MNRAS, 265, 301
Smolec, R. 2005, AcA, 55, 59
Soszy'nski, I., Udalski, A., Szyma'nski, M.K. et al. 2014, AcA, 64, 177
Storm, J., Nordström, B., Carney, B.W., Andersen, J. 1994, A&A, 291, 121
Storm, J., Carney, B.W., Latham, D.W., Davis, R.J., & Laird, J.B. 1992, PASP, 104, 168
Sumi, T. et al. 2004, MNRAS, 348, 1439
Suntzeff, N.B., Kinman, T.D. & Kraft R.P. 1991, ApJ, 367, 528
Tumlinson, J. 2010, ApJ, 708, 1398
Walker, A.R. 1989, PASP, 101, 570
Walker, A.R. & Terndrup, D.M. 1991, ApJ, 378, 119
Wallerstein, G. Gomez, T. & Huang, W. 2012, Ap&SS, 341, 89
Zoccali, M. et al. 2008, A&A, 486, 177
Zoccali, M. et al. 2014, A&A, 562, 66